Electronic Supplementary Material (ESI) for Journal of Materials Chemistry A.

Supporting Information

A novel open architecture built by ultra-fine single-crystal $Co_2(CO_3)(OH)_2$ nanowires and reduced graphene oxide for asymmetric supercapacitor

Xuning Leng [a], Libo Wu [a], Yan Liu [b], Chunlin Li [a], Sufeng Wei [c], Zhonghao Jiang [a], Guoyong Wang [a,*], Jianshe Lian [a], and Qing Jiang[a]

[a] Key Laboratory of Automobile Materials, Department of Materials Science and Engineering, Jilin University, No. 5988 Renmin Street, Changchun 130025, PR China

[b] Key Laboratory of Bionic Engineering (Ministry of Education), Jilin University, Changchun 130025, PR China

[c] Key Laboratory of Advanced Structural Materials, Changchun University of Technology, Changchun 130012, PR China

* Corresponding author. E-mail addresses: materwanggy@jlu.edu.cn, Tel: +86 431 85095875; Fax: +86 431 85095876.

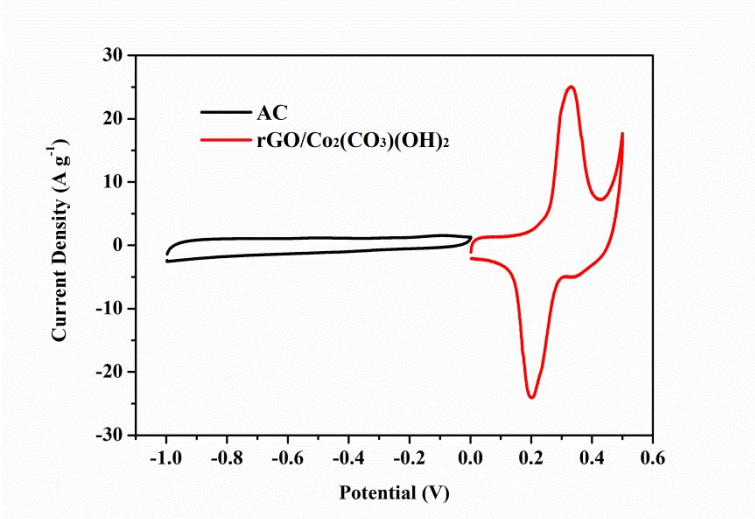

Fig. S1 Comparative CV curves of $rGO/Co_2(CO_3)(OH)_2$ and activated carbon (AC) electrodes performed in a three-electrode configuration at a scan rate of 10 mV s^{-1}.

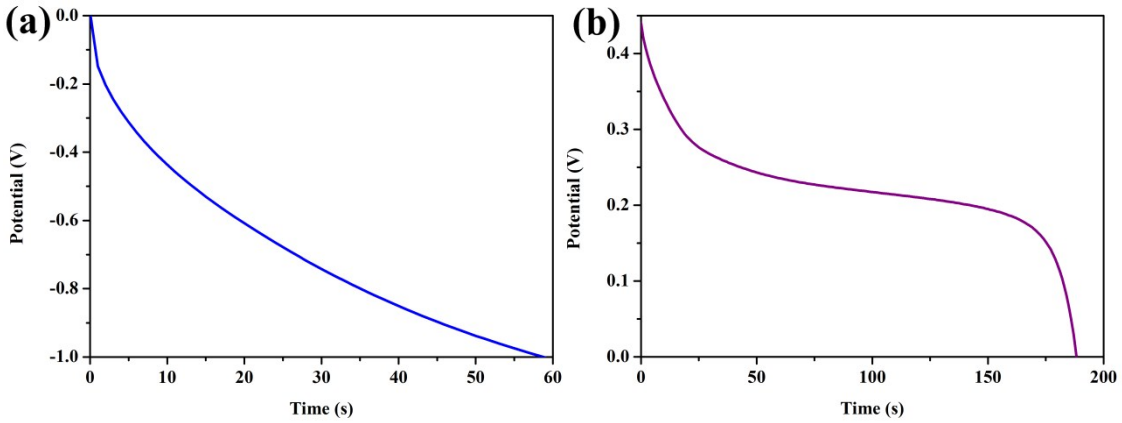

Fig. S2 Galvanostatic discharge curves of the AC electrode (a) and $rGO/Co_2(CO_3)(OH)_2$ electrode (b) at a current density of 2 A g^{-1} in a three-electrode cell with saturated calomel reference electrode in 3 M KOH electrolyte.

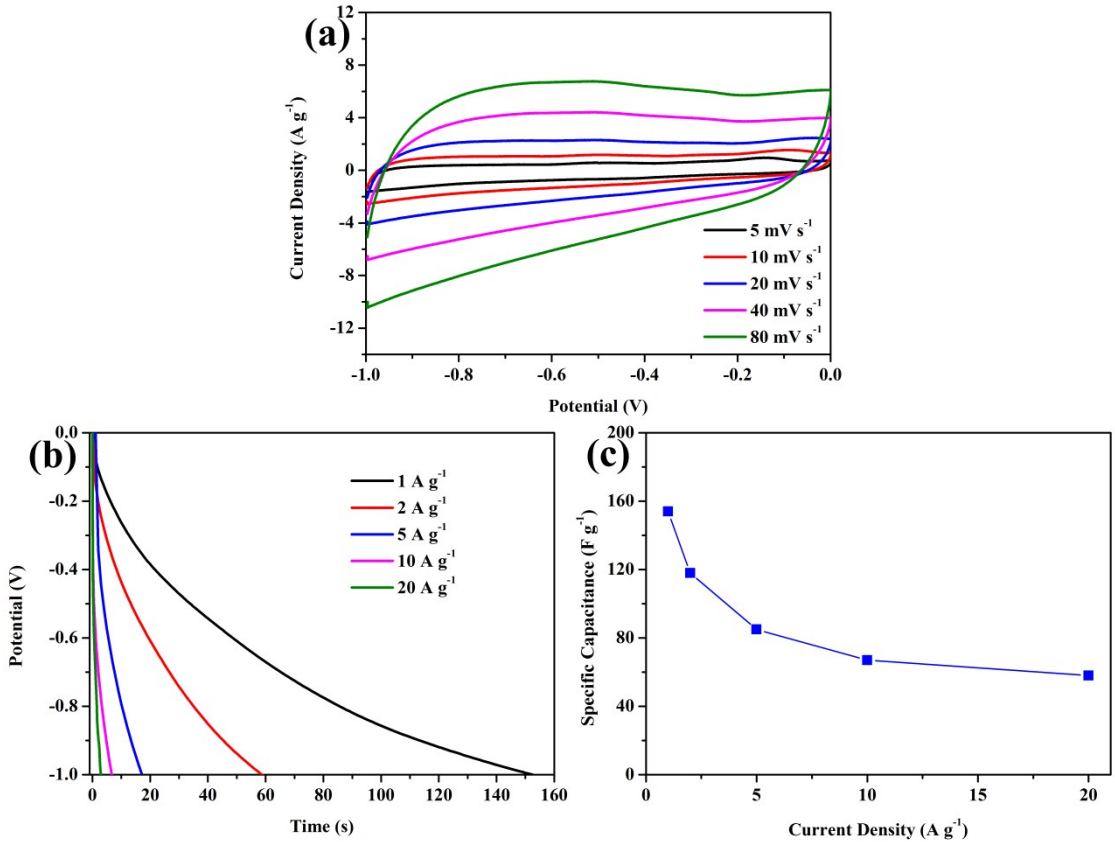

Fig. S3 (a) CV curves, (b) galvanostatic discharge curves of the AC electrode at different current densities in 3 M KOH, and (c) specific capacitance of AC as a function of current densities.

As shown in CV curves (Fig. S3a), AC electrode exhibits the typical rectangular shapes from 0 to –1 V without a significant distortion even at a high scan rate of 80 mV s^{-1}. According to the discharge curves (Fig. S3b) using the formula: $C_s = I \cdot \Delta t \cdot m^{-1} \cdot \Delta U^{-1}$, the AC electrode shows specific capacitance values of 154, 118, 85, 67, and 58 F g^{-1} at current densities of 1, 2, 5, 10, and 20 A g^{-1}, respectively (Fig. S3c).

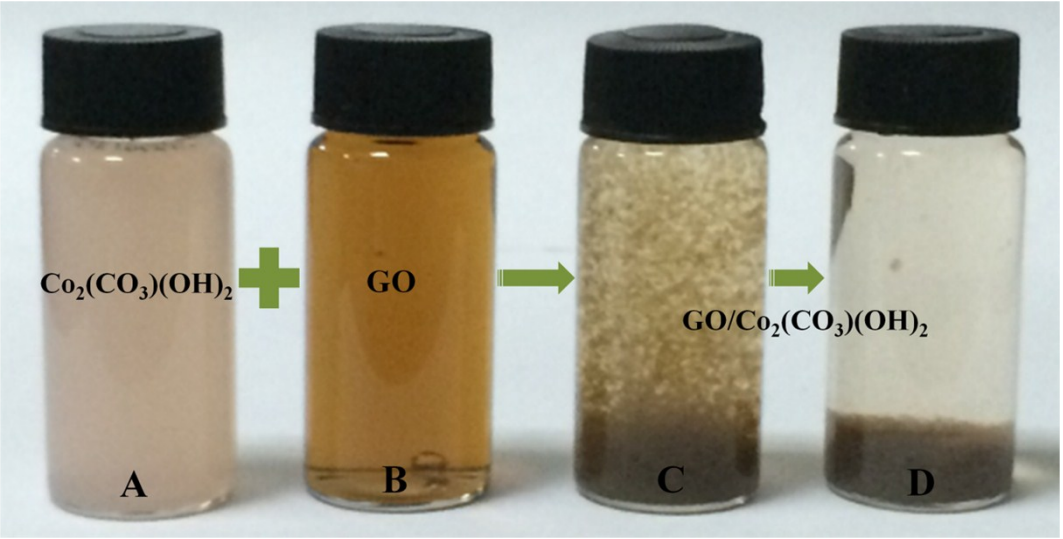

Fig. S4 Photographs of the co-assembly process of GO and $Co_2(CO_3)(OH)_2$ in the aqueous solutions.

A: $Co_2(CO_3)(OH)_2$ aqueous solution. $Co_2(CO_3)(OH)_2$ nanowires could uniformly disperse in deionized water for 0.5 h;

B: GO aqueous solution. Graphite oxide was uniformly dispersed in deionized water, forming brown GO solution;

C: $GO/Co_2(CO_3)(OH)_2$ aqueous solution. GO aqueous solution (B) was slowly dropped in $Co_2(CO_3)(OH)_2$ aqueous solution (A) and stirred for seconds. It can be found aggregation of $Co_2(CO_3)(OH)_2$ nanowires and GO in this photograph, indicating the successful assembly between GO and $Co_2(CO_3)(OH)_2$ nanowires;

D: $GO/Co_2(CO_3)(OH)_2$ aqueous solution after washed with de-ionized water. A puce precipitate was accumulating in the bottom and supernatant solution is completely colorless and transparent, concluding that almost all $Co_2(CO_3)(OH)_2$ nanowires are homogeneously dispersed onto the surface of the GO sheets.

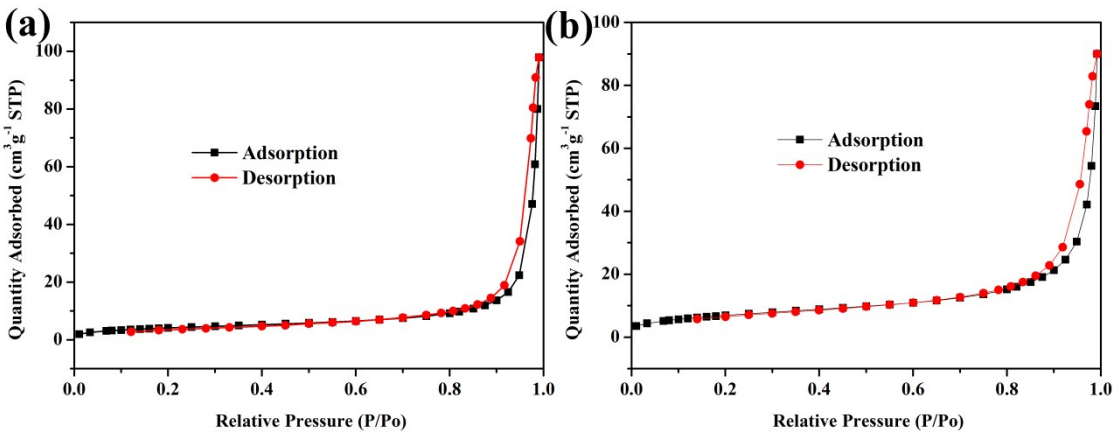

Fig. S5 Nitrogen adsorption/desorption isotherms of (a) the pure $Co_2(CO_3)(OH)_2$ nanowires and (b) the rGO/$Co_2(CO_3)(OH)_2$ composite.

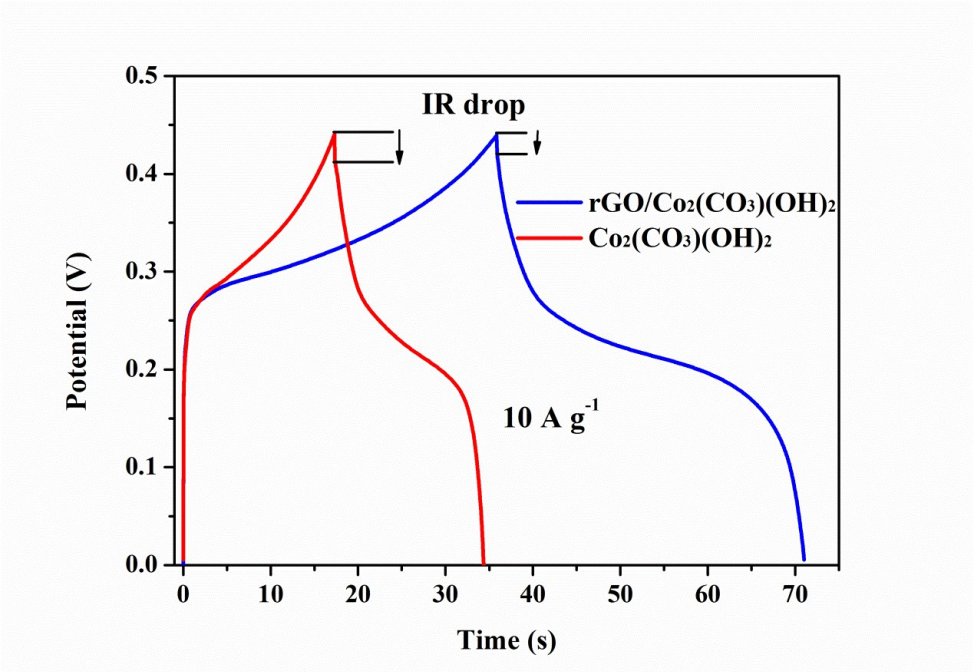

Fig. S6 GCD profiles of rGO/$Co_2(CO_3)(OH)_2$ and $Co_2(CO_3)(OH)_2$ at a current density of 10 A g^{-1}.

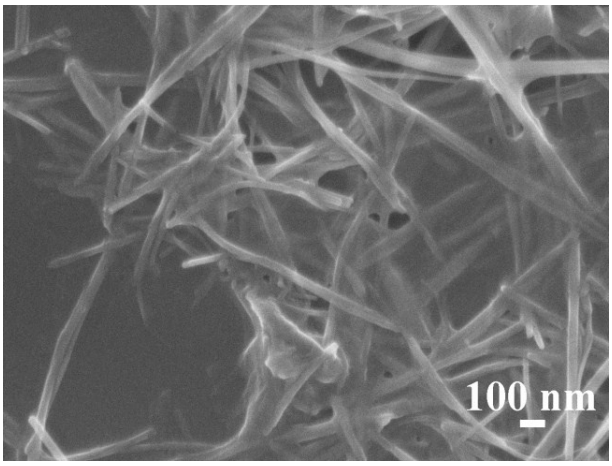

Fig. S7 FESEM image of rGO/$Co_2(CO_3)(OH)_2$ electrode after cycling. The unique architecture, that is, both $Co_2(CO_3)(OH)_2$ nanowires and rGO sheets supporting each other, is kept after the long cycles, indicating the excellent stability.